Simulation of effects of vegetation on the dispersion of pollutants in street canyons

KAI RIES[1] and JOACHIM EICHHORN[2]

[1]Lahmeyer International GmbH, Bad Vilbel, Germany
[2]Institut für Physik der Atmosphäre, Johannes Gutenberg-Universität, Mainz, Germany

(Manuscript received December 15, 2000; accepted , 2001)

Abstract

An extension of the numerical model MISCAM to account for effects of vegetation is presented. Computed wind and turbulence profiles agree reasonably with wind tunnel data. Furthermore, the extended model yields plausible results for flow fields and pollutant distributions in an idealized street canyon with and without vegetation. While wind speed is reduced within the vegetated street canyon, a slight increase of pollutant concentrations is found.

Zusammenfassung

Eine Erweiterung des numerischen Modells MISKAM zur Behandlung von Vegetationseinflüssen wird vorgestellt. Berechnete Wind- und Turbulenzprofile stimmen zufriedenstellend mit Windkanaldaten überein. Darüber hinaus liefert das erweiterte Modell plausible Ergebnisse für die Strömungs- und Ausbreitungsverhältnisse in einer idealisierten Straßenschlucht mit und ohne Vegetation. Während die Windgeschwindigkeit bei vorhandener Vegetation abnimmt, wird ein geringfügiger Anstieg der Schadstoffkonzentrationen simuliert.

1 Introduction

The numerical microscale model MISCAM has been developed to model specific flow and dispersal conditions in urban built-up areas. Up to now, the influence of vegetation on wind and turbulence distributions has been accounted for in a rather approximative way utilizing the roughness length. This method, however, does not realistically reproduce wind profiles within tree stands, which are characterized by a significant slow down within the crowns and a moderate reduction of wind speed below.

The subject of the present study is the extension of the model equations in terms of additional drag forces, which quantify vegetation effects depending on the density of the stand as well as the distribution of leaf areas. Several model runs have been carried out for a built-up roadway to demonstrate the influence of vegetation on mass concentrations. Results are in qualitative agreement with the findings of GROSS (1997), who implemented a similar scheme to the microscale model ASMUS. Quantitative comparisons of model results and field observations will be presented in a forthcoming paper. The range of applications of MISCAM is significantly improved by the current model extensions. For example, rows of trees or partly porous obstacles can be modeled in a more realistic way by prescribing suitable values of the vegetation parameters.

[1] Address: Corresponding author: Kai Ries, Lahmeyer International GmbH, Friedberger Straße 173, 61118 Bad Vilbel, Germany, e-mail: ge_117@lif.de

2 The Model

The prognostic system of MISCAM consists of the cartesian components of the equation of motion using the anelastic Boussinesq approximation. Buoyancy effects, however, are neglected as well as the Coriolis force. The basic set of dynamic equation reads

$$\frac{\partial u_i}{\partial t} + \frac{\partial u_n u_i}{\partial x_n} = \frac{\partial}{\partial x_n}\left[K_m\left(\frac{\partial u_i}{\partial x_n} + \frac{\partial u_n}{\partial x_i}\right)\right] - \frac{1}{\rho}\frac{\partial p}{\partial x_j} \tag{2.1}$$

$$\frac{\partial u_n}{\partial x_n} = 0 \tag{2.2}$$

Additionally, a poisson type equation for the dynamic pressure perturbations must be solved to ensure mass conservation. The pressure correction is carried out by use of the well-known splitting scheme of PATRINOS and KISTLER (1977). Once wind and turbulence distributions have been computed, the transport equation for chemically inert tracers

$$\frac{\partial c}{\partial t} + \frac{\partial u_j c}{\partial x_j} = \frac{\partial}{\partial x_n}\left[K_h \frac{\partial c}{\partial x_n}\right] + Q_c \tag{2.3}$$

may be solved to give a three-dimensional distribution of the mass concentration c of a nonreactive gas.

Diffusion coefficients are computed from a E-ε-closure which is described in some detail in EICHHORN (1996). In the present study, for reasons of simplicity, the dissipation rate ε is obtained diagnositically from the turbulence kinetic energy and a mixing length. The latter is computed from the usual BLACKADAR (1962) formula where the height is replaced by the minimum distance to the solid model boundary.

At inflow boundaries, pre-calculated profiles of wind components and turbulence variables are kept constant in time. No-flux conditions are used for outflow boundaries with an additional pressure correction applied to ensure mass conservation throughout the model domain.

Within the numerical implementation the advection processes are handled by an upstream-discretization. For mass transport optionally up to two corrective steps to reduce numerical diffusion (SMOLARKIEWICZ and GRABOWSKI, 1989) may be applied. Diffusion equations for both momentum and mass concentrations are solved by means of the ADI algorithm of DOUGLAS and RACHFORD (1956). A simple SOR method is adopted to solve the Poisson equation for the dynamic pressure disturbance.

In the model buildings are explicitly taken into account as three-dimensional rectangular obstacles. A complete description of the discretization scheme as well as the numerical procedures is given by EICHHORN (1989).

3 Treatment of Vegetation

The main effects of vegetation on the flow regime near the ground are a reduction of wind speed as well as increased turbulence within the tree crowns. These effects are incorporated in the model equations by use of an additional drag force which is given as (see WILSON and SHAW, 1977):

$$F_{veg,i} = \rho n_c c_d b u_i |\vec{u}| \tag{3.1}$$

with the stand density n_c and the leaf area density b. c_d is a drag coefficient resulting from the slowing down of the flow due to momentum exchange with the vegetation. According to GROSS (1993), it is specified as $c_d = c_{d0} n_c^2$ with $c_{d0} = 0.2$. The stand density is given as the surface fraction covered by the vertical projection of the vegetation. Typical horizontal grid resolutions of MISCAM are small (≈ 2 m), therefore values of either 0 (no vegetation) or 1 (grid cell completely covered with vegetation) have been used in the examples described lateron. The extended model equations are the equation of motion and the equation for the turbulent kinetic energy:

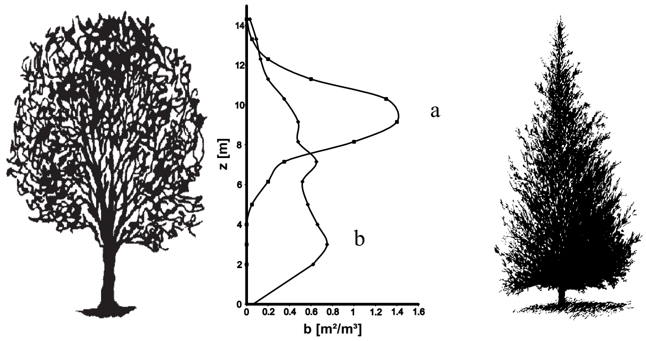

Figure 1: Typical vertical profiles of the leaf area density of (a) deciduous trees (RAUNER, 1976) and (b) coniferous (HICKS et al., 1975).

$$\left.\frac{\partial u_i}{\partial t}\right|_{veg} = \left.\frac{\partial u_i}{\partial t}\right|_{old} - \frac{1}{\rho} F_{veg,i} \tag{3.2}$$

$$\left.\frac{\partial E}{\partial t}\right|_{veg} = \left.\frac{\partial E}{\partial t}\right|_{old} + n_c c_d b |\vec{u}|^3 \tag{3.3}$$

The leaf area density, defined as the projected leaf area per unit volume, depends on the vegetation type as well as the season. Vertical profiles for deciduous trees show a maximum within the crown while for coniferous trees with a conical silhouette the maximum is located noticeable lower. Typical profiles are shown in Figure 1.

The stand density n_c must be determined by either extraction from topographical maps or satellite data or, for small scale studies as typical applications of MISCAM, by a direct inspection of the model area. Values for b have to be estimated, considering the type of vegetation under concern. Measured values are gathered by GROSS (1993).

4 First Results

Various sensitivity studies have been carried out with the extended model. For example, the flow through different types of tree stands (deciduous or coniferous trees) were simulated, as well as flow and pollutant dispersal within a vegetated street canyon.

4.1 Comparison with wind tunnel data

First, a model run for coniferous trees has been used to examine the quality of model results in comparison to wind tunnel data (Green, 1992). The total extensions of the model configuration are 6000 m in x- and 200 m in z-direction. The tree stand extends from 500 m $\leq x \leq$ 700 m with a height h of 20 m. Inflow is from the left with a wind speed of 6 m s^{-1} at a height of 100 m.

The original mixing length formula gave poor results for turbulent kinetic energy, although the wind profiles are in good agreement with the observations. As can be seen from Figure 2, turbulence level is way too high within the tree stand. By limiting the mixing length to

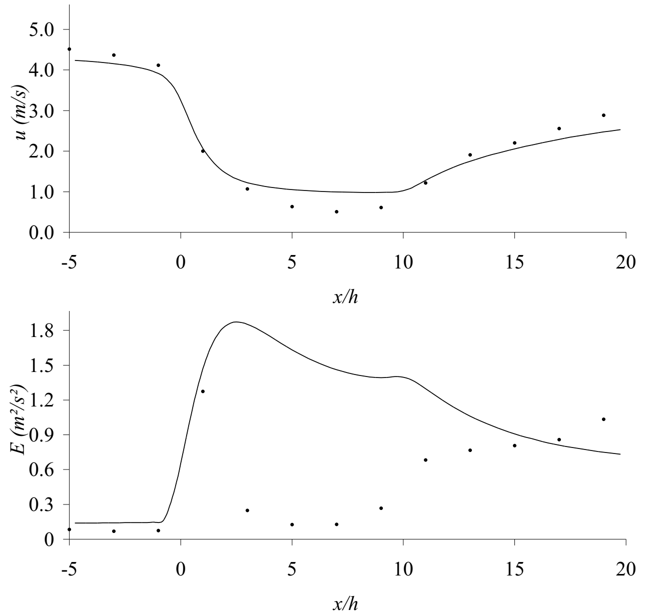

Figure 2: Horizontal profiles of wind speed and turbulence energy at $z/h = 0.75$ for flow simulation with original mixing length formula. — MISCAM results, · · · wind tunnel data

the grid distance within vegetated grid cells, the model behaviour improved noticeably (Figure 3, 4). Nevertheless, there are still obvious discrepancies between model results and measurements, especially downstream of the tree stand ($x/h > 10$) and above the canopy. Because of the overall better model performance, for the simulations discussed below the modified mixing length formula has been adopted.

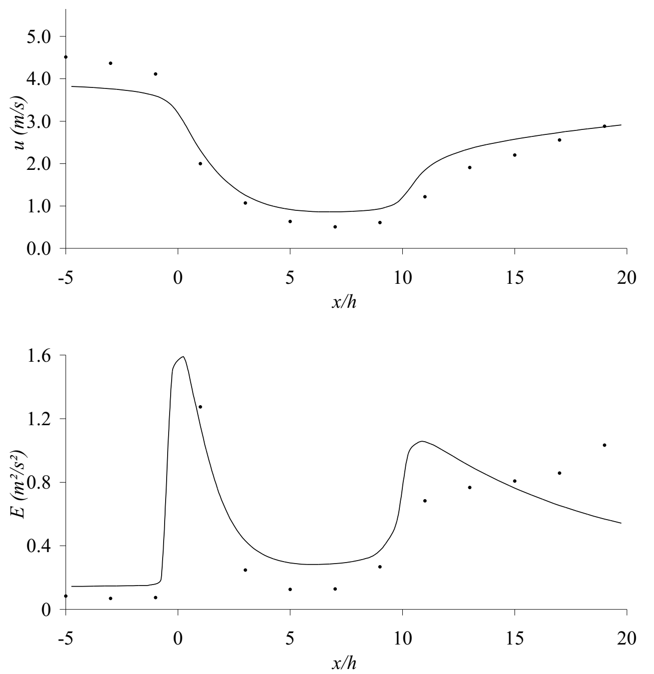

Figure 3: As in Figure 2, but with modified mixing length formula

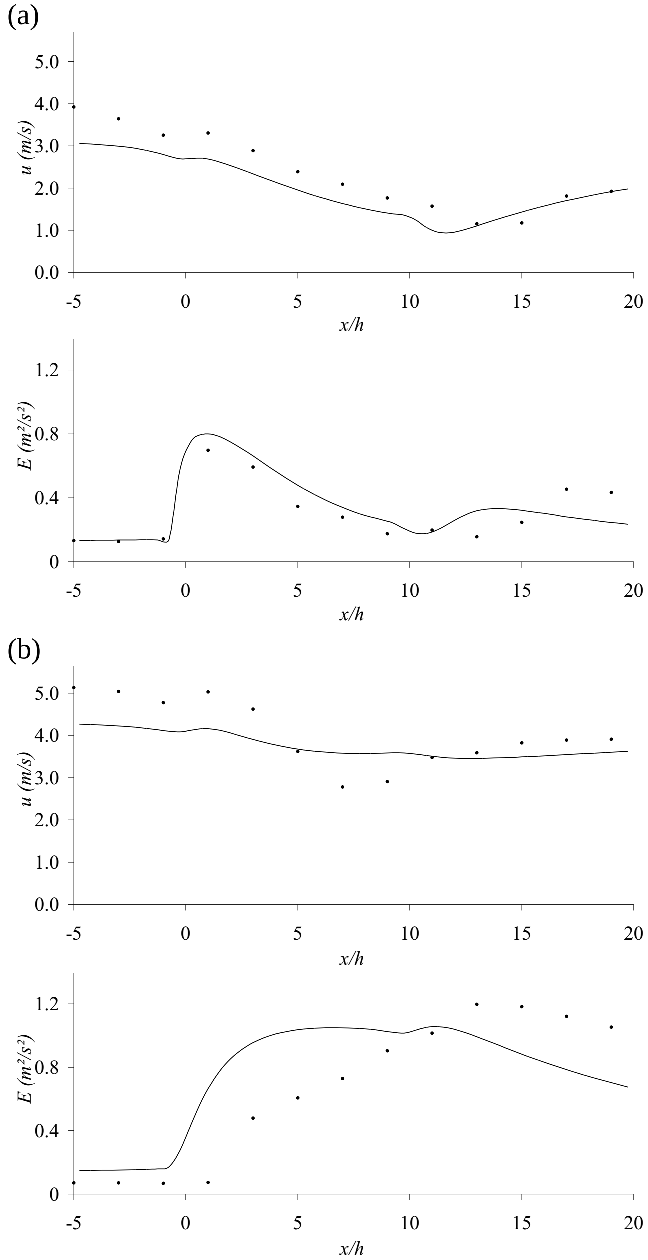

Figure 4: As in Figure 3, but for $z/h = 0.25$ (a) and $z/h = 1.25$ (b)

4.2 Flow through different types of vegetation

Next, the model run has been repeated for deciduous trees. Figure 5 shows vertical cross sections of the flow fields in terms of normalized velocities $u(x,z)/u(0,z)$ for both vegetation types.

Within the tree crowns, in both cases, wind speed is significantly reduced. For coniferous trees, however, the speed reduction follows the vertical profile of b with a stronger effect near the ground. In both cases the tree crowns act as slightly porous flow obstacles, with a larger portion of the flow being redirected above and below the crowns of deciduous trees. This leeds to a less pronounced Bernoulli like flow within the stem zone accompanied by an increased downstream influence in case of coniferous trees.

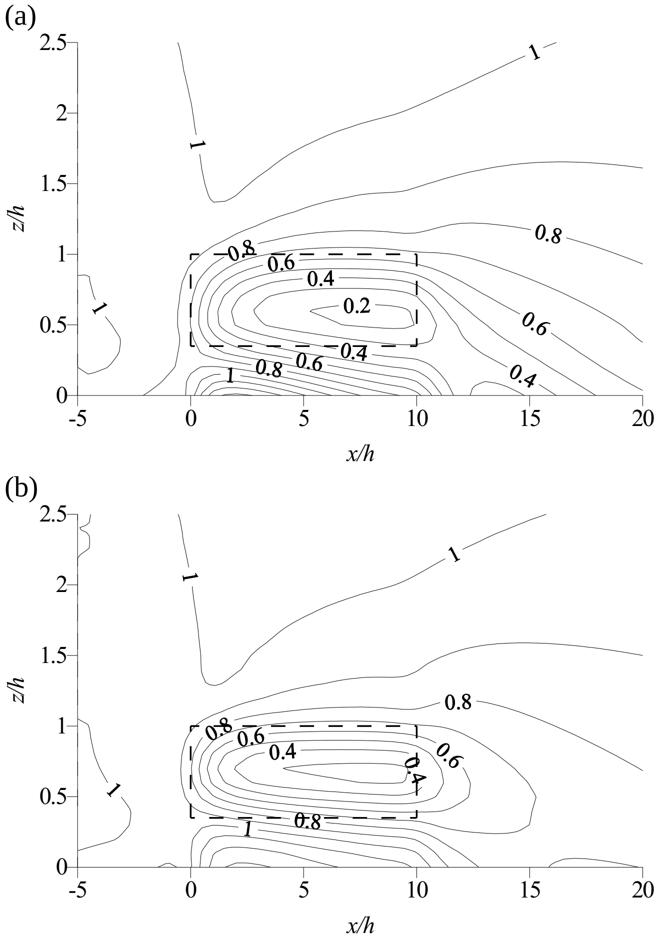

Figure 5: Normalized wind speed for flow through tree stand consisting of coniferous trees (a) and deciduous trees (b)

4.3 Flow and pollutant dispersal in a street canyon

Some flow and dispersal simulations for an idealised two-dimensional street canyon will be discussed next. Figure 6 shows the model configuration, consisting of a street canyon of 30 m width and with a height of 14 m. The total model extensions are 92 m in *x*- and 90 m in *z*-direction with a resolution of 2 m.

Rows of trees are placed on both sides of the roadway. Leaf area density and stand density have been chosen to represent typical deciduous trees (RAUNER, 1976) whose crowns completely cover the respective grid cells. The simulations have been run twice, once with and once without inclusion of the trees.

In Figures 7 and 8, the resulting changes of wind speed and mass concentrations are given. As indicated in Figure 6, inflow is from the left with a wind speed of 5 m s^{-1} at a height of 10 m. The dotted line indicates the position of the tree crowns within the model grid.

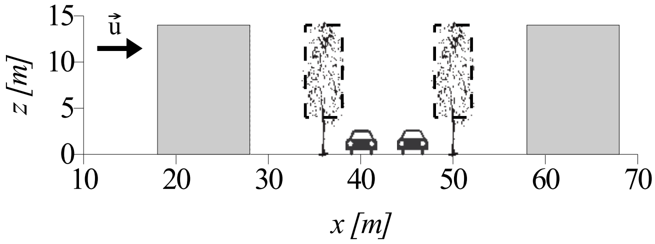

Figure 6: Scetch of model configuration. Shaded surfaces represent buildings, inflow direction is indicated by arrow. The car symbols indicate the positions of line sources.

Overall effects are small, wind speed is reduced by up to 4 cm s^{-1} near the ground and within the tree crowns. The maximum percental reduction due to the inclusion of the trees reaches 10 % within the tree crowns. A slight Bernoulli like acceleration of 2 – 3 cm s^{-1} in the central parts as well as the rightmost parts of the street canyon is noted where the flow is redirected around the tree crowns. The percental increase amounts to approximately 12 % in the central parts of the canyon.

A source strength of 10 μg $m^{-1}s^{-1}$ of an arbitrary gas has been specified, yielding maximum concentrations of roughly 10 μg m^{-3} in the left part of the street canyon. Approximately, this source intesity can be identified as the emission of carbon monoxide resulting from a stream of 40.000 cars per day.

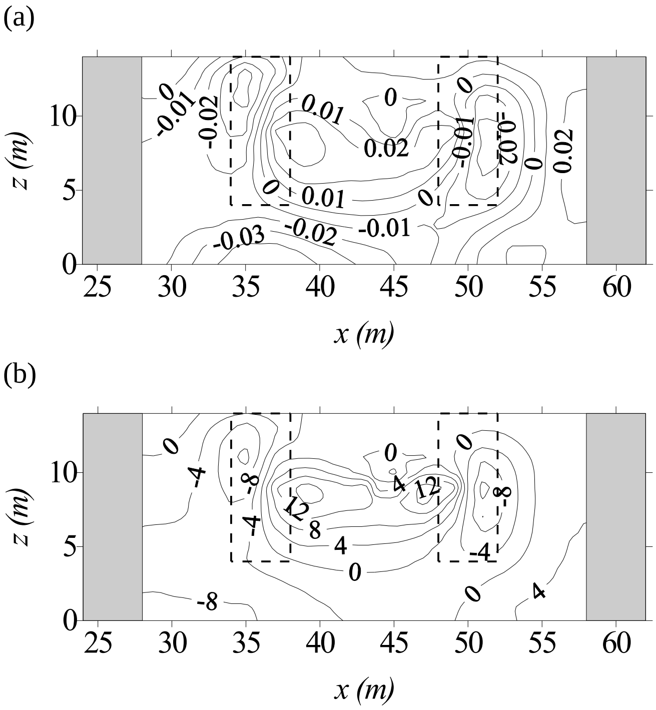

Figure 7: Wind speed change in (m s^{-1}) (a) and percental change (b) due to vegetation.

As a result of decreased wind speed, pollutant concentrations near the ground are slightly higher in case

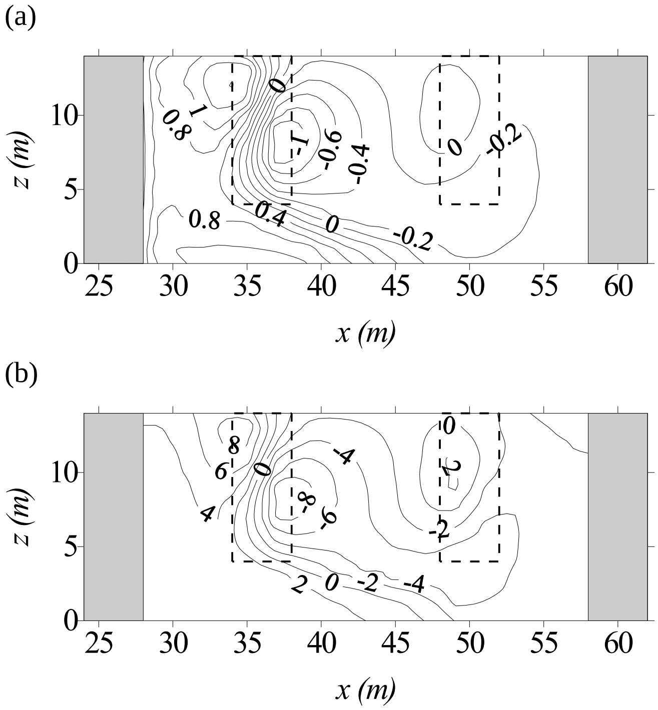

Figure 8: Change of pollutant concentration (μg cm^{-3}) (a) and percental change (b) due to vegetation.

of the vegetated street canyon. Concentrations between the tree rows are lower in comparison to the model run without trees, since a greater portion of the released gas is kept in the area below the crowns. The maximum increase of concentration amounts to 1.2 μg m^{-3}, means 8 %, of the original values, which is in qualitative accordance to results of Gross (1997) who also found that higher mass concentrations due to vegetation effects are restricted to the lee side of the street canyon.

Additional computations have been run for alternate canyon geometries and leaf area distributions. In case of a narrower canyon (width 18 m) with very dense tree crowns situated next to the building walls, the increase of mass concentrations near the ground amounts to 20 % of the values without vegetation.

5 Conclusions

The current study represents a new chapter of the steady further development of MISCAM. Results of the extended model show an acceptable agreement with wind tunnel data for flow through a small tree stand. Nevertheless, the defects of the E-l-closure for the turbulence-system is obvious. Therefore, the next indispensable step will be the inclusion of the complete E-ε-closure.

However, first sensitivity studies are encouraging for future work on MISCAM. Both, the wind and flow fields in an idealised street canyon show the expected behaviour due to the incorporation of vegetation, in this case rows of trees on both sides of the roadway. Wind speed is reduced within the tree crowns and, as a consequence, pollutant concentrations within the leeward portions are slightly higher in case of the vegetated street canyon.

References

BLACKADAR, A.K. 1962: The vertical distribution of wind and turbulent exchange in a neutral atmosphere, J. Geophys. Research, **67**, 3095-3102

DOUGLAS, J., H. RACHFORD 1956: On the Solution of heat conduction problems in two and three space variables. - Trans. Amer. Mat. Soc., **82**, 421-439

EICHHORN, J. 1989: Entwicklung und Anwendung eines dreidimensionalen mikroskaligen Stadtklimamodells. - PhD thesis, Universität Mainz.

EICHHORN, J. 1996: Validation of a microscale pollution dispersal model. - In: Air Pollution Modeling and Its Application XI, Plenum Publishing Corporation, New York, U.S.A., 539-548.

GROSS, G. 1993: Numerical Simulation of Canopoy Flows. - Springer Series in Physical Environment, **12**, Springer, Berlin.

GROSS, G. 1997: ASMUS - Ein numerisches Modell zur Berechnung der Strömung und der Schadstoffverteilung im Bereich einzelner Gebäude. II: Schadstoffausbreitung und Anwendung. - Meteorol. Z., N.F. **6**, 130-136.

HICKS, B.B., P. HYSON, C.J. MOORE 1975: A study of eddy fluxes over a forrest. - J. Appl. Met., **14**, 58-66

PATRINOS, A.N.A., KISTLER, A.L. 1977: A numerical Study of the Chicago lake breeze. - Boundary Layer Meteor., **12**, 93-123

RAUNER, J.L. 1976: Deciduous Forests. - In: J. L. Monteith (ed.) Vegetation and the Atmosphere, Vol. 2, Academic Press, New York, U.S.A., 241-264.

SMOLARKIEWICZ, P.K., GRABOWSKI, W.W. 1989: The multidmensional positive definite advection transport algorithm: nonoscillatory option. - J. Comput. Physics, **86**, 355-375

WILSON, N.R., R.H. SHAW 1977: A higher order closure model for canopy flow. - J. Appl. Met., **16**, 1197-1205.